JOURNAL OF MATERIALS SCIENCE 30 (1995) 2577–2583

Fracture mechanisms and particle shape formation during size reduction of a model food material

M. G. SCANLON
Department of Food Science, University of Manitoba, Winnipeg, Manitoba, Canada R3T 2N2
J. LAMB
Procter Department of Food Science, University of Leeds, Woodhouse Lane, Leeds, LS2 9JT, UK

The importance of particle shape to powder properties warrants examination of the effect of size reduction on particle shape formation. In this study, a model food material (dried gelatinized starch) was comminuted in an impact breakage gun, a hammer mill (with and without a screen) and in a blender. After sieving, particle shape at selected sizes was assessed as deviation from sphericity. Generally, particle shapes were elongated at smaller size, except for those produced by unscreened hammer milling. Particle shapes were unaffected by impact velocity in the gun, but were rounded by increased milling. Fractography was used to demonstrate how elongated particles formed. During fracture, fracture fronts were disturbed by air holes in the material, creating cleavage steps. Subsequent undercutting of the steps as fracture planes spread released the elongated particles. Such particle formation mechanisms may account for anomalous size distribution results at early stages of grinding. Particle shape differences between mills and single impact breakage were ascribed to particle selection mechanisms surmised to be operating in the mill. Both material properties and the size reduction method were shown to affect particle shape, thus fracture progress in a given material should be studied if particles of specific shapes are to be produced by comminution.

1. Introduction

Sizes and shapes of particles formed during size reduction processes depend on how fracture paths ran through the original stressed material. Many studies have been devoted to investigations of the size of particles resulting from comminution [1–3], but as noted by Holt [4], particle shape formation during comminution has received relatively little attention. This is despite improvements in imaging and computing techniques which have made measurement and analysis of particle shape easier [5], and despite the importance of particle shape to the technological properties of collections of comminuted particles.

In the construction of highways the shapes of crushed aggregate particles in asphalt determine the ability of the asphalt to withstand loading without permanent deformation [6]; the more irregular the shapes of the aggregate particles, the more stable the asphalt [7]. In the fabrication of polymeric composite materials the shapes of filler particles (which may be produced by comminution) have a marked effect on the rheological properties of the composite [8]. In pneumatic conveying of particles, wear on structures is more severe if particles are angular in shape [9]. Other examples which illustrate the importance of particle shape arising from comminution have been provided by Durney and Meloy [10].

The effect of particle shape on technological properties is no less pronounced when the comminuted particles are of recent biological origin. In creating fibreboards, the shape of comminuted wood particles dictates the breakage load of the fibreboard if density is maintained at a constant level [11]. The capacity of particulate foods to disperse upon wetting (a desirable attribute in "instant" food powders) is also dependent on particle shape [12]. Storage and flowability problems of foods and feedstuffs are strongly influenced by the shape of comminuted particles [13], a prime example being the shape difference between particles created from milling of hard and soft wheats [14]. The irregular shapes of soft wheat particles hinders flowability, lowering flour production capacity when milling soft wheats [15], and so increasing unit costs.

This study investigated particle shapes arising from comminution of a model food material [16] in two impact mills. An impact breakage gun was also employed for size reduction, so that the effect of particle selection would not contribute to the mechanics of shape formation in progeny particles [17]. Fracture surfaces were examined to ascertain whether

propagating fractures interacted with structural features of the food material to produce specific particle shapes.

2. Experimental procedure

2.1. Material

As described previously [18] comminution analyses were performed on an essentially isotropic and brittle material, composed of a biopolymer (starch) that is commonly found in food materials that are subjected to size reduction [16]. Although essentially isotropic, under microscopic examination small pores were seen to be distributed throughout the material, presumably an artefact of the drying stage. Slabs of the dried material were cut into approximately 8.0 mm cubes using a band saw with a blade of 0.645 mm width, prior to size reduction by any of the methods.

2.2. Mills and impact breakage gun

Full descriptions of the methods of size reduction of collections of particles, and of single impact breakage of individual particles have been previously reported [18]. Briefly these were: a sharp bladed mill (blender) operated dry for 100, 200, 400 and 800 s; a fixed-hammer hammer mill that was used with and without a screen, the product from one milling becoming the feed material for the next milling, up to a total of five passes; and a compressed air gun (eductor) which directed individual particles at three impact velocities (40, 68 and 85 ms^{-1}) onto a breaker plate inside a padded particle collection chamber.

All particles were collected prior to size and shape analysis. Since particle shape was not analysed for all particle size analyses, the number of replicates was different from that given previously [18]. For the blender, there were nine replicates for 100 s milling, three for 200 s milling and two for 400 and 800 s milling. The number of replicates for each velocity in the impact breakage gun, each pass in screened and unscreened hammer milling were six, three and three, respectively, but no shape analyses were performed for the fourth run of the screened and unscreened hammer millings.

2.3. Shape analysis

Particles were separated on a $(2^{0.5})$-geometric progression of sieves from 32 μm to 8.0 mm using a test sieve shaker run for 10 min.

As the particles ranged in size from 8.0 mm downwards, a rapid and easy way of measuring particle shape over a wide range of sizes was required. To cover the whole range of sizes and to reduce operator error, virtual images of the particles were projected onto a screen by means of apparatus similar to that employed by Needham and Hill [19]. In this study an overhead projector was used as the light source. Light collected from the projector by a hood shone through a transparent stage which was just below the projector lens. Particles were placed on the stage and a removable lens fixture inserted between the stage and the projector lens. One or two lenses were inserted in the fixture to increase magnification, depending on particle size. To create images of 5600 μm particles the hood was removed and the particles placed on the deck of the overhead projector.

As the purpose of shape examination was to compare shapes at different sizes and millings, a convenient method was a modification of Riley's sphericity [20], so that the shape factor was defined as

$$\phi_0^2 = i/D$$

where D is the diameter of the smallest circle which just circumscribes the perimeter of the particle lying on its maximum cross-sectional area (assumed), and i the diameter of the largest inscribed circle which will fit in the profile. These two diameters were measured on the image of each selected particle by using a small piece of perspex on which was inscribed concentric circles at 2 mm intervals. It was moved manually over the particle image to obtain i and D.

The sieves chosen to assess particle shape were 90–125, 250–355, 710–1000, 2000–2800 and 5600–8000 μm if particles were present at these sizes. Fifteen to twenty particles were chosen from a fixed random pattern. Although the statistical validity of this is questionable [21], choosing samples of 50 and 600 particles did not decrease the standard deviation for ϕ_0^2 when compared with samples of fifteen from the same source; nor did the number of particles used for the determination of ϕ_0^2 significantly alter the mean value.

2.4. Fractography

A Kyowa (Tokyo) stereoscopic microscope using incident light was used to examine fracture surfaces of larger pieces of broken cubes. Breakage was performed for one impact in the blender by starting the blender and then dropping a cube onto the blades and catching the progeny particles in a large plastic bag positioned where the lid normally was. Large particles were also examined from cubes that had been broken in the gun at low and intermediate impact velocities.

Photomicrographs of these fracture surfaces were taken with a Nikon Optiphot apparatus using incident light from a quartz halogen fibre optic illuminator.

2.5. Statistical analysis

An analysis of variance was performed on particle shape data using the general linear models (GLM) procedure of SAS, Version 6.07 (SAS Institute Inc., Cary, NC). The analysis was carried out separately on each of the four size reduction methods (blender, impact gun, screened and unscreened hammer milling), the purpose being to elucidate differences between particle shape for the various sizes and treatments. Treatments for the gun were impact velocities; for the blender, time of milling; and for the hammer mill, number of passes. The significance of any differences between means arising from the analysis of variance was tested by paired t- test comparisons.

3. Results

3.1. Impact gun

Differences between mean ϕ_0^2 values at different impact velocities were small (0.53–0.51), and were not consistent with a hypothesis that increasing velocity (or energy) was responsible for formation of specific particle shapes [22, 23], since the order of decreasing particle shape was 40, 85 and 68 ms^{-1}.

Differences in values of ϕ_0^2 with changes in impact velocity were small when compared with changes in ϕ_0^2 for different particle sizes (Fig. 1). The decrease in sphericity as particle size decreased indicated the presence of more elongated particles at smaller sizes. It can be seen that for a given velocity mean ϕ_0^2 values for many sieve sizes were significantly different from mean ϕ_0^2 values on other sieves. Overall, ϕ_0^2 values (particle shapes) were highly significantly ($p < 0.001$) dependent on particle size.

3.2. Unscreened hammer mill

Increased passes of material through the mill almost effected a ranking of ϕ_0^2 values according to the number of passes; values of ϕ_0^2 decreased in the order of: pass five > pass three > pass one > pass two. Differences in ϕ_0^2 were small, being 0.66 for pass five compared with 0.61 for pass two. However, averaged over all the sieve sizes, differences between ϕ_0^2 values for pass five and some of the other passes were significantly different, even up to the 0.1% level.

Table I shows mean values of ϕ_0^2 on the selected sieves. As with breakage in the gun, ϕ_0^2 was greatest for the 5600 μm sieve and least for the 90 μm sieve. However, on the intermediate sieves ϕ_0^2 values were not ordered as they were in the gun. It is also noteworthy that the difference in ϕ_0^2 between 5600 and 90 μm particles was 0.06, a small difference when compared with a mean difference of 0.24 for particles produced by impact inthe gun. As noted by Scanlon and Lamb [18], there were two differences between unscreened hammer milling and impact breakage at 85 ms^{-1}: first, the effect of particle selection in the mill must be considered, and second, secondary breakage of fractured particles can occur on the metal casing of the mill. These two differences are obviously great enough that shapes of the resulting particulate distribution are dissimilar to those generated in the gun.

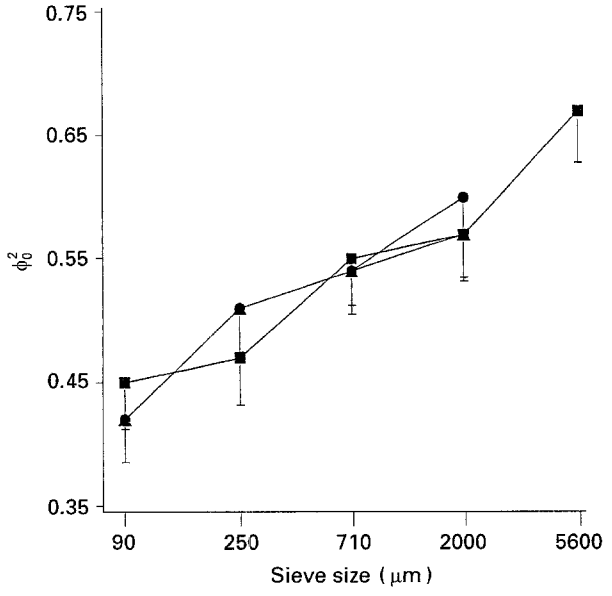

Figure 1 Changes in particle shape, ϕ_0^2, on lower sieve sizes for particles produced in the impact breakage gun at impact velocities of 40 (■), 68 (▲) and 85 ms^{-1} (●). Error bars are ± 95% confidence limit.

TABLE I Shapes of particles produced by unscreened hammer milling. Values are means of passes one to three and five and three replicates. [a,b] Means denoted by same letter are not significantly different at 5% level

Sieve size (μm)	Mean ϕ_0^2 value
5600	0.67[a]
250	0.65[a]
2000	0.62[b]
710	0.61[b]
90	0.61[b]

TABLE II Shapes of particles produced by screened hammer milling. Values are means of passes one to three and five and three replicates. [a–c] Means denoted by same letters in first superscript are not significantly different at 5% level; in second superscript at 0.1% level.

Sieve size (μm)	Mean ϕ_0^2 value
710	0.66[a,a]
250	0.63[b,a]
90	0.58[c,b]

3.3. Screened hammer mill

The addition of a screen to the hammer mill produced some differences in particle shape compared to unscreened hammer milling. Mean values of ϕ_0^2 increased as the number of passes through the mill increased. The magnitude of change in shape from pass five to pass one was greater (0.66–0.57, respectively) than for milling without the screen, but significant differences in shape were only seen for particles from pass one compared to particles produced by other passes ($p < 0.001$).

Table II shows shape differences between the three sieves where particles were present. Unlike hammer milling without the screen, the value of ϕ_0^2 fell as particle size decreased, following the pattern shown for impact breakage in the gun. However, the magnitude of the decrease was not as great as in the gun, and indeed, although all size fractions had significantly different particle shapes from each other at the 5% level, only the 90 μm particles were different in shape from other sizes at the 0.1% level.

3.4. Blender mill

The action of the blender mill is unlike the other three methods of impact size reduction in that the area of impacting surface on the particles is small, generating a less uniform distribution of stresses within the

TABLE III Changes in particle shape with time of blender milling. Values are means for the number of replicates (Section 2.2) and for all selected sieve sizes. [a–c]Means denoted by same letter are not significantly different at the 5% level.

Time of milling (s)	Mean ϕ_0^2 value
800	0.64[a]
400	0.60[b]
200	0.59[b]
100	0.57[c]

TABLE IV Shapes of particles produced by blender milling. Values are means of replicates (see Section 2.2) and of the four milling times. [a–c]Means denoted by same letters are not significantly different at 5 or 0.1% levels.

Sieve size (μm)	Mean ϕ_0^2 value
2000	0.65[a]
710	0.63[a]
250	0.56[b]
90	0.49[c]

particle. It would therefore be expected that the resulting particle shapes would be different from the other three methods of size reduction [23]. As time of milling increased, mean values of ϕ_0^2 increased (Table III), indicating more rounded particle shapes. Differences between ϕ_0^2 noted in Table III disappeared as the level of significance decreased, such that at the 0.1% level, significant differences in particle shapes were only seen between 800 and 200, and 800 and 100 millings.

The change in ϕ_0^2 with particle size is shown in Table IV. The trend was similar to that seen for the impact gun: particle shape was more elongated at smaller size. The magnitude of the change in ϕ_0^2 with size was also similar to that of the gun: 0.31 for 5600–90 μm (0.24 for the gun) and 0.16 for 2000–90 μm (0.15 for the gun). In the case of the blender, when any given sieve was examined, mean ϕ_0^2 values were higher than for the gun.

4. Discussion

4.1. General considerations

The results of particle shape versus size for the unscreened hammer mill appear to be an anomaly, since all other forms of size reduction showed decreases in ϕ_0^2 as size decreased, implying the presence of more elongated particles at smaller sizes. The majority of the results therefore substantiate Allen's observation [21] that materials of the same composition do not have the same shape throughout their size range. The production of greater numbers of elongated particles by size reduction at smaller sizes has been noted by a number of researchers [10, 23–26]. It was also observed in this study that the standard deviation associated with the mean value of ϕ_0^2 for a given sieve increased as size decreased for all modes of size reduction except the unscreened hammer mill. The increase (although not statistically significant) was particularly noticeable for the 90 μm sieve. This observation implies a greater heterogeneity in particle shapes at smaller sizes.

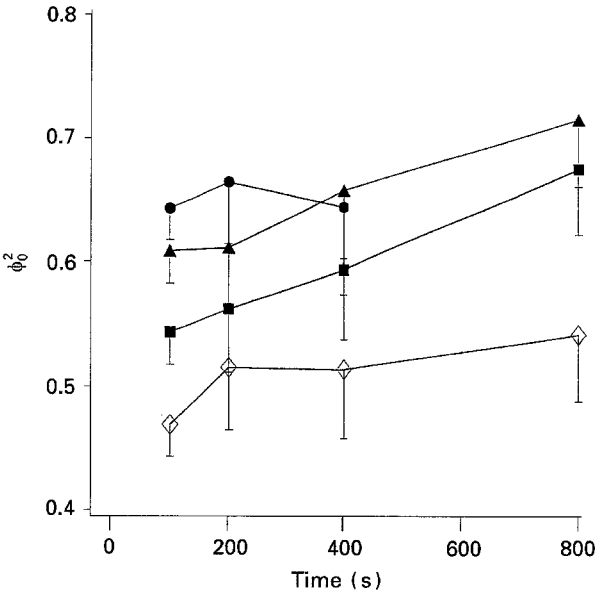

Figure 2 Changes in particle shape, ϕ_0^2, with time of blender milling for particles on sieve sizes of 2000 (●), 710 (▲), 250 (■) and 90 μm (◇). Error bars are ± 95% confidence limit.

When considering how particle shape changes with increased milling the results for size reduction in the unscreened hammer mill concur with the results for blender and screened hammer milling: with few exceptions, as the degree of milling increased, particle shapes at any given particle size became more rounded. Fig. 2 illustrates this effect for blender milling. Changes in particle shape with increased amounts of grinding have been demonstrated [25, 27] including a decrease in the number of elongated particles [28, 29], although the latter effect was not observed in grinding of Soma sand [26].

According to theoretical considerations [23], substantiated by the photographic observations of Charles [22], the lower velocity and thinner blade of the blender should initiate fracture from fewer flaws and thus produce greater numbers of elongated particles. The results of blender milling support such observations. However, the patterns of stresses which are generated in particles by high velocity impacts, such as breakage by the gun and hammer milling (without or with the screen), should be the same. Particles produced by the gun and by hammer milling with the screen had a pattern of particle shape versus particle size that was closer to that of the blender, making interpretation of these results according to Holt's theory [23] and Charles' observations [22] difficult. Also, since particle shapes produced by 85 and 40 ms^{-1} impact in the breakage gun showed no major differences in shape, it appears that an alternative explanation for particle formation is required. In seeking such an explanation concentration on events occurring in the breakage gun is helpful, since this method of size reduction is free of secondary breakage and selection effects in the mill [17, 30].

4.2. Particle shapes generated by impact breakage gun

Particle shapes will be related to the way in which cracks ran through the original stressed material [29].

At the crack tip a strong stress concentration provides the elastic energy necessary to maintain fracture [31]. Since interaction of the crack tip stress field with inhomogeneities causes complex wave phenomena which affect crack propagation and direction [32], it was thought that material inhomogeneity (the presence of pores) could change stress patterns as the crack propagated. This phenomenon might then be responsible for the production of elongated particles of low ϕ_0^2 values at smaller sizes, which theoretically should not arise from crack trajectories resulting from impact loading of a homogeneous material [23].

Examination of the fracture surfaces of large particles did indeed show evidence of interaction between the pores and an advancing crack. Fig. 3 shows the result of a fracture which moved from left to right, met one of the pores (which disturbed the stress field at the tip of the crack) and caused fracture to continue on two planes. The presence of two fracture planes caused a cleavage step to be present where the two planes meet, a phenomenon reported to occur during fracture of metals [33], glass [34], rocks [34], silicon [35], magnesium oxide [36], various organic polymers [33, 37–40] and extruded wheat starch plasticized with glucose and water [41, 42]. Fig. 4 is a magnification of the same pore in Fig. 3. It is apparent that the lower fracture plane was formed to the left of the pore (top of figure), while the upper fracture plane was formed on meeting the pore. The propagation of the fracture front into different cleavage planes as a result of fracture front stress waves interacting with pores [43, 44] and other material inhomogeneities [36, 37, 45] has been previously reported. The large pore size in this material permits the right-hand side of the lower fracture plane (bottom of Figs. 3 and 4) to be visible through the thin distance separating upper and lower fracture planes. It is therefore apparent that an undercutting has occurred at the cleavage step as a result of brittle fracture, similar to that proposed by Preston [34] and Swain *et al.* [35]. Cleavage step formation and undercutting would thus be expected to proceed as shown in Fig. 5, so that a sliver of this elongated material would form during the fracture process.

Independence of the slivers formed from the main fracture face has previously been reported [39, 42, 46], and is substantiated for this material in Fig. 6, where two fracture planes have intersected approximately at right angles. The right-angle plane cut has occurred at a different point on the overhanging sliver than on the fracture plane on which it was lying. The number of elongated particles formed will depend solely on the number of fracture faces, with the number of slivers formed on each fracture face being proportional to the number of pores which the propagating fracture encounters. Therefore, it is expected that large numbers of these particles would be generated by impact in the breakage gun, regardless of impact velocity. Values of ϕ_0^2 would thus be lowered on the 250 and 90 μm sieves, on which most of the slivers formed by this fracture mechanism would reside. The presence of elongated

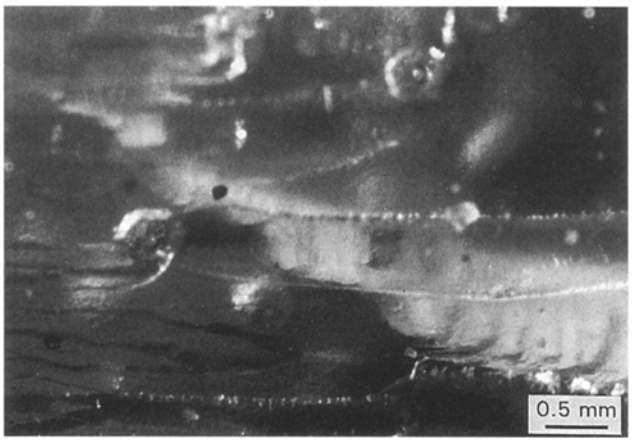

Figure 3 Cleavage step formation and production of elongated particle resulting from fracture plane (moving from left to right) meeting pore.

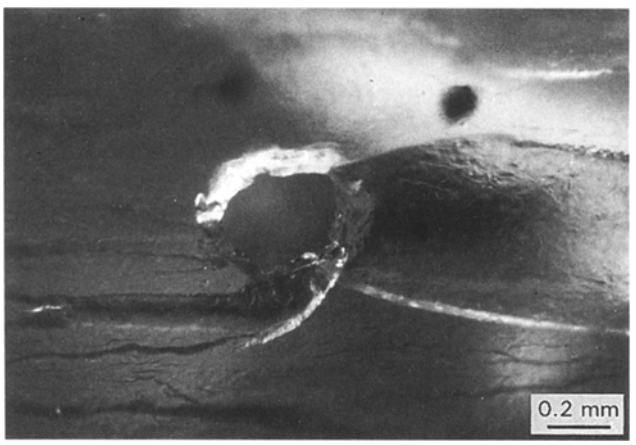

Figure 4 Magnification of pore in Fig. 3 showing cleavage step initiation.

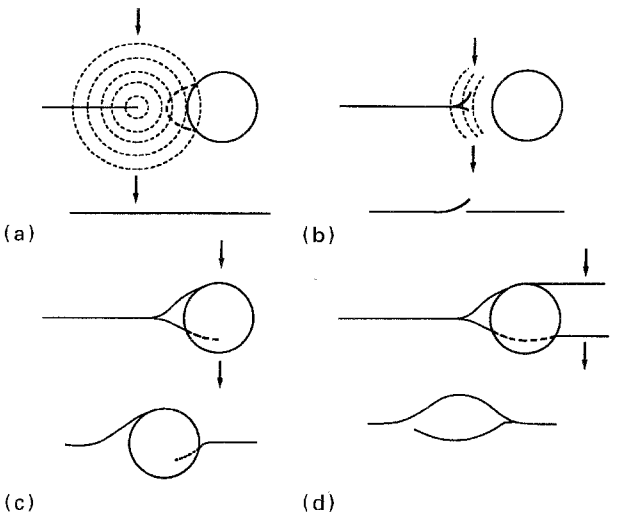

Figure 5 Cleavage plane formation and overlap during four stages of crack propagation. Bottom diagrams are sections of the fracture plane drawn perpendicular to advancing fracture front at the point of vertical arrows in top diagrams. (a) Advancing fracture moving left to right with stress waves emanating from tip of crack. (b) Reflected stress waves disturb fracture front causing crack bifurcation. (c) Crack branch continues to deviate from original fracture plane due to further stress waves reflection from the pore. (d) Main fracture plane spreads outwards and undercuts fracture plane of crack branch thereby creating a sliver that will create an elongated particle.

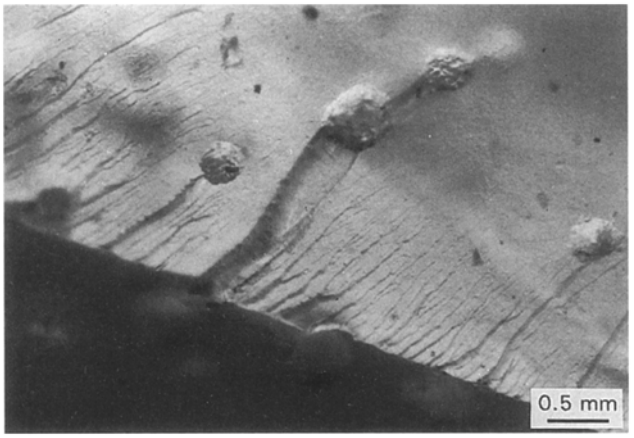

Figure 6 Intersection of two fracture planes, approximately at right angles, showing elongated particle being fractured at a different point to the fracture plane on which it was residing.

particles admixed with particles reduced in size by "more normal" fracture processes [47, 48] would account for the observed increase in the standard deviation for ϕ_0^2 at smaller sizes, since there are essentially two mechanisms for particle formation at smaller sizes. The almost perfect isotropicity of glasses would limit the number of inhomogeneities, so that under impact fracture conditions blocky shaped particles were produced [22, 23, 48], contrary to these results.

4.3. Particle shapes generated in the hammer mill

Regardless of the presence or absence of the screen, fracture mechanisms occurring in particles that are hammer milled would be expected to be similar to those occurring in the impact breakage gun at 85 ms^{-1}. However, in the hammer mill the effect of particle selection in the mill [17] and secondary breakage [49] must be considered. These factors obviously influence fracture events to the extent that shape distributions versus size are markedly different from those arising from single impact breakage.

4.3.1. Unscreened hammer mill

The effects of any impact from the hammers should produce from the fracture surfaces the same elongated particles as were formed in the gun. But, in the hammer mill the close proximity of the surrounding metal casing ensures that kinetic energy derived from fracture is used in secondary breakage [49]. As elongated particles would be unlikely to break along their longest axis the particles formed from secondary breakage of any slivers would be more blocky than elongated [10]. The observation of twice as much material formed below 355 μm for the unscreened hammer mill compared with impact breakage at 85 ms^{-1} [18] implies that considerable secondary breakage has occurred. The more rounded shapes of the products of secondary breakage would then increase ϕ_0^2 values at smaller sizes accounting for the results in Table I.

4.3.2. Screened hammer mill

The above effects of secondary breakage on particle shape would be expected to be more pronounced when a screen was added. However, ϕ_0^2 decreased with decreasing particle size, contrary to the effect observed in hammer milling without a screen. When milling glass, Holt [23] also saw increased numbers of elongated particles of size range 125–250 μm when a screen was added to a hammer mill, and elongated particles were observed in screened hammer milling of Soma sand in the 40–150 μm size range [26]. The addition of the screen causes an extra selection effect that is size dependent, so that particles that would normally pass into the bag unaltered in unscreened hammer milling are retained on the screen. The strong outward air currents in the mill would blow out particles smaller than the screen aperture, generally the smaller elongated particles. Larger particles are retained to be rebroken. The relative number of these preferential selection events occurring on the screen (and expulsion of elongated particles) determines how much the mean value of ϕ_0^2 is lowered at smaller sizes compared to hammer milling without the screen. Additional lowering of ϕ_0^2 due to the screen would be expected from particles that have been broken and the kinetic energy associated with the progeny particles causes secondary breakage on the screen rather than on the upper casing. In this case any slivers formed during this secondary breakage would likely be ejected from the mill, and not subject to further breakage which would increase their ϕ_0^2 values.

4.4. Particle shapes generated in the blender mill

A single impact of a particle by the blender blade does not effect the same degree of size reduction as does impact in the hammer mill or in the gun (even at low velocity). Therefore fewer fracture surfaces and their concomitant slivers will be produced. The slivers will dominate the particulate population at small sizes leading to low ϕ_0^2 values, while at larger sizes, values of ϕ_0^2 will be high due to the blocky shaped particles that are produced. This will be particularly so when time of grinding is small.

The presence of elongated slivers could account for the creation of small particles (fines) in the early stages of grinding whose mass is independent of the mass of material being ground [50]. This is because the number of elongated fines created will be proportional to the new fracture surface area. New fracture surface area will be dependent solely on material that has been selected for breakage, and unless the mill is grossly underloaded this will be independent of mass of material in the mill. The presence of "badly shaped particles" in the fines of crushed rocks [51] could arise from a similar fracture mechanism to the one shown to operate in this study, since generation of elongated slivers on rock fracture faces has been reported [34].

As the time of milling in the blender is increased, ϕ_0^2 increased for all sizes. The slivers which are produced and which continue to be available for breakage in such a closed system would likely fracture across

their short axes forming more blocky shapes [10]. Increasing ϕ_0^2 values as the number of passes in the hammer mill increased would likely be due to a similar mechanism: smaller elongated particles returned for milling preferentially fracturing across their short axes, so increasing ϕ_0^2 values.

5. Conclusions

Particles of elongated shape were present at small particle sizes resulting from impact breakage at three velocities and in two different impact mills. This is contrary to the findings of other researchers who found impact breakage produced mainly rounded particles. Material inhomogeneity (the presence of small pores) was responsible for the result. As fractures propagated, stress field interaction with the pores caused cleavage step formation. Undercutting of these cleavage steps caused small particles of elongated shape to be liberated, increasing the numbers of elongated particles at lower sizes. Breakage of these elongated particles across their long axes was responsible for the fall in number of these particles as time of blender milling, or number of passes in the hammer mill, increased. Differences in the shape versus size distribution between material hammer milled with or without a screen was surmised to be due to the manner in which particles were selected for rebreakage within the mill.

Acknowledgements

The authors would like to thank Dr O. Flint and Mr H. Zimberg for help with the photographs, Dr T. Hughes and Mr J. Elliot in the Department of Metallurgy (Leeds) for help in the calibration of impact gun velocities, R. Roller for assistance with the statistical analyses, and especially Mr Philip Nelson for skilful construction of the impact gun. The authors are grateful for a Research grant (1981–84) from the Science and Engineering Research Council, as part of the Specially Promoted Programme on Particulate Technology, and for partial funding from the Canadian Natural Sciences and Engineering Research Council.

References

1. B. BEKE, "Principles of Comminution" (Akadémiai Kiadó, Budapest, 1964).
2. A. M. GAUDIN, *Trans. AIME* **73** (1926) 253.
3. G. C. LOWRISON, "Crushing and Grinding" (Butterworths, London, 1974).
4. C.B. HOLT, *Powder Technol.* **28** (1981) 59.
5. J. K. BEDDOW, "Particle Size Distribution: Assessment and Characterization", ACS Symposium Series 332 (American Chemical Society, Washington, DC, 1987) p. 2.
6. W. R. MEIER JR and E. J. ELNICKY, *Transp. Res. Rec.* **1250** (1989) 25.
7. I. ISHAI and H. GELBER, *Asphalt Paving Technol.* **51** (1982) 494.
8. N. S. ENIKOLOPYAN, M. L. FRIDMAN, I. O. STALNOVA and V. L. POPOV, *Adv. Polym. Sci.* **96** (1990) 1.
9. I. M. HUTCHINGS, *Chem. Engng Sci.* **42** (1987) 869.
10. T. E. DURNEY and T. P. MELOY, *Int. J. Miner. Process.* **16** (1986) 109.
11. H. TAKAHASHI, H. SUZUKI and K. ENDOH, *Tappi*, **62**(7) (1979) 85.
12. H. SCHUBERT, *J. Food Engng* **6** (1987) 1.
13. E. HEIDENREICH and G. MULLER, *Chem. Tech.* (Leipzig) **41** (1989) 24.
14. D. V. NEEL and R. C. HOSENEY, *Cereal Chem.* **61** (1984) 259.
15. M. NUSSBAUMER, *Buhler Diagram* **96** (1990) 19.
16. J. LAMB and M. G. SCANLON, *J. Mater. Sci. Lett.* **4** (1985) 1296.
17. A. W. P. G. PETERS RIT, M. HAGG and J. VAN BRAKEL, "Powtech '83 Particle Technology", IChE Symposium 69 (Institute of Chemical Engineers, Rugby, 1983) p. 1.
18. M. G. SCANLON and J. LAMB, *Powder Technol.* **74** (1993) 279.
19. L. W. NEEDHAM and N. W. HILL, *Fuel Sci. Pract.* **14** (1935) 222.
20. N. A. RILEY, *J. Sediment. Petrol.* **11** (1941) 94.
21. T. ALLEN, "Particle Size Measurement", 3rd edn, (Chapman & Hall, London, 1981).
22. R. J. CHARLES, *Min. Eng.* (NY) **8** (1956) 1028.
23. C. B. HOLT, "Particle Technology", IChE Symposium 63 (Institute of Chemical Engineers, Rugby, 1981) p. D2/H/1.
24. C C. HARRIS and G. STAMBOLTZIS *Powder Technol.* **2** (1968) 58.
25. R. ROUSSEV and P. SOMASUNDARAN, *Part. Sci. Technol.* **4** (1986) 305.
26. Y. KUGA, X. MA, J. KOGA, S. ENDOH and I. INOUE, *Powder Technol.* **44** (1985) 281.
27. S. BANISI, A. R. LAPLANTE and J. MAROIS, *CIM Bull.* **84** (955) (1991) 72.
28. J. M. LYTLE and K. A. PRISBREY, *Powder Technol.* **38** (1984) 93.
29. M. ABOUKHESHEM, K. PRISBREY, L. R. BUNNELL and J. M. LYTLE, *Part. Sci. Technol.* **4** (1986) 143.
30. K. R. YUREGIR, M. GHADIRI and R. CLIFT, *Chem. Engng. Sci.* **42** (1987) 843.
31. H. SCHARDIN, in "Fracture, Proceedings of an International Conference on Atomistic Mechanisms of Fracture", edited by B. L. Averback, D. K. Felbeck, G. T. Jahn and D. A. Thomas (Massachusetts Institute of Technology & Wiley, New York, 1959) p. 297.
32. P. S. THEOCARIS, *Engng Fract. Mech.* **15** (1981) 283.
33. J. A. KIES, A. M. SULLIVAN and G. R. IRWIN, *J. Appl. Phys.* **21** (1950) 716.
34. F. W. PRESTON, *J. Amer. Ceram. Soc.* **14** (1931) 419.
35. M. V. SWAIN, B. R. LAWN and S. J. BURNS, *J. Mater. Sci.* **9** (1974) 175.
36. F. F. LANGE and K. A. D. LAMBE, *Phil. Mag.* **18** (1968) 129.
37. A. C. MOLONEY and H. H. KAUSCH, *J. Mater. Sci. Lett.* **4** (1985) 289.
38. A. CHRISTIANSEN and J. B. SHORTALL, *J. Mater. Sci.* **11** (1976) 1113.
39. B. W. CHERRY and K. W. THOMSON, *ibid.* **16** (1981) 1925.
40. M. ATSUTA and D. T. TURNER, *J. Mater. Sci. Lett.* **1** (1982) 167.
41. A.-L. OLLETT, R. PARKER and A. C. SMITH, in "Food Polymers, Gels and Colloids", edited by E. Dickinson (Royal Society of Chemistry, Cambridge, 1991) p. 537.
42. *Idem, J. Mater. Sci.* **26** (1991) 1351.
43. R. L. COBLE and N. M. PARIKH, in "Fracture: An Advanced Treatise", Vol. 7, edited by H. Liebowitz (Academic, New York, 1972) p. 243.
44. N. SHINKAI and H. SAKATA, *J. Mater. Sci.* **13** (1978) 415.
45. C. M. AGRAWAL, K. HUNTER, G. W. PEARSALL and R. W. HENKENS, *ibid.* **27** (1992) 2606.
46. J. D. VENABLES, *J. Appl. Phys.* **31** (1960) 1503.
47. E. F. PONCELET, *Trans. AIME* **169** (1946) 37.
48. W. J. MECHAM, L. J. JARDINE, G. T. REEDY and M. J. STEINDLER, *Ind. Eng. Chem. Fundam.* **22** (1983) 384.
49. B. H. BERGSTROM and C. L. SOLLENBERGER, *Trans. AIME* **220** (1961) 273.
50. C. C. HARRIS, *ibid.* **241** (1968) 359.
51. F. A. SHERGOLD, *J. Soc. Chem. Ind. Trans.* **65** (1946) 245.

Received 11 April
and accepted 31 October 1994